

## **Models for Estimating the Deformation Capacities of Reinforced Concrete Columns**

M. Inel

*Pamukkale University, Department of Civil Engineering, Denizli 20020, Turkey*

M. A. Aschheim

*Mid-America Earthquake Center, University of Illinois at Urbana-Champaign, Urbana, IL 61801-2352, USA*

**ABSTRACT:** Five models for estimating deformation capacity of RC columns are reviewed in an attempt to establish reliable inelastic displacement capacities. Displacement ductility, peak drift, and plastic hinge rotation parameters are used as measures of inelastic deformation. In many cases the analytical models are observed to overestimate deformation capacity and exaggerate the effect of transverse steel on deformation capacities. A simple, classical model is shown to produce similar or better estimates of the column deformation capacities than more complex models.

**Keywords:** deformation capacity, reinforced concrete columns, displacement ductility

**ÖZET:** Betonarme kolonların deformasyon kapasitelerini elde etmek amacıyla mevcut beş ayrı model incelenmiştir. Elastic ötesi deformasyon ölçütü olarak yer değiştirme sünekliliği, maksimum öteleme ve plastic mafsallık dönme parametreleri kullanılmıştır. Birçok durumda analitik modellerin yüksek yer değiştirme kapasiteleri verdiği ve enine donatının deformasyon kapasiteleri üzerindeki etkiyi olduğundan fazla gösterdiği gözlenmiştir. Daha karmaşık modellere oranla, basit ve klasik bir modelle benzer veya daha iyi kolon deformasyon kapasitelerinin hesaplanabileceği gösterilmiştir.

### **Introduction**

Inelastic behavior is intended in most structures subjected to infrequent earthquake loading. Reinforced concrete columns are the preferred locations of inelastic behavior in many bridges because of their accessibility for inspection and repair. Thus, the development of displacement-based design procedures for bridges requires knowledge of the deformation capacity of the bridge columns.

Methods for estimating the deformation capacity of reinforced concrete columns have been the focus of many research studies. Several available models for estimating column deformation capacity include those by Park and Paulay (1975), Lehman and Moehle (1998), Panagiotakos and Fardis (2001), and Priestley et al. (1996). Except for the empirical model of Panagiotakos and Fardis (2001), these models estimate the

deformation capacity at yielding and ultimate based on lumped inelasticity idealization for a cantilever, as shown in Figure 1. The simplest form of such model is to compute deformation capacities based on flexural contributions, assuming the curvature distributions of Figure 1, as described by Park and Paulay in 1975. This approach is termed the “simple” model in this paper.

This paper reviews five analytical models in an attempt to establish reliable deformation capacities. Displacement ductility, drift, and plastic hinge rotation parameters are used as measure of inelastic deformation. A limited set of experimental data from large-scale tests of reinforced concrete columns having a rectangular cross section are also considered. Estimates of the deformation capacities of the columns are compared to the observed deformation capacities. Nominal deformation capacities for columns with reinforcement as recommended by ATC-32 (Improved Seismic Design Criteria for California Bridges) are suggested based on the experimental data.

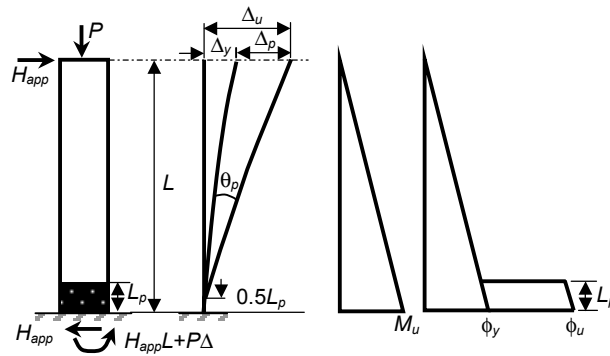


Figure 1. Lumped inelasticity model for a cantilever column

## Evaluation of Inelastic Deformation Capacities

The load-deformation behavior of a column is commonly idealized by a bilinear curve that is fit to the response computed analytically, or may be fitted approximately to the envelope of experimental test results. Although a bilinear curve may be defined by two points, the yield and ultimate displacements ( $\Delta_y$  and  $\Delta_u$ ) and the corresponding loads, various definitions of these points have been used by different researchers. Once the yield and ultimate points are established, the displacement ductility,  $\mu_\delta$ , plastic displacement,  $\Delta_p$ , plastic hinge rotation,  $\theta_p$ , and peak drift,  $\delta_d$  capacities may be derived for the cantilever column of Figure 1.

$$\mu_\delta = \frac{\Delta_u}{\Delta_y} \quad (1)$$

$$\Delta_p = \Delta_u - \Delta_y \quad (2)$$

$$\theta_p = \frac{\Delta_u - \Delta_y}{L - 0.5L_p} \quad (3)$$

$$\delta_d = \frac{\Delta_u}{L} \quad (4)$$

While experimental data is invaluable without doubt, the design of columns normally relies on calculated estimates of the load-deformation behavior, as illustrated in Figure 2. The yield and ultimate displacements may be estimated by including the contributions of flexure, shear, and anchorage slip, as proposed by various researchers.

$$\Delta_y = \Delta_{y,flexure} + \Delta_{y,slip} + \Delta_{y,shear} \quad (5)$$

$$\Delta_u = \Delta_{u,flexure} + \Delta_{u,slip} + \Delta_{u,shear} \quad (6)$$

The five models considered in this paper are: (1) “simple” model, (2) Lehman model (Lehman and Moehle, 1998), (3) Panagiotakos analytical model (Panagiotakos and Fardis, 2001), (4) Panagiotakos empirical model (Panagiotakos and Fardis, 2001), and (5) Priestley model (Priestley et al., 1996). The calculation of yield and ultimate displacements according to the five models is summarized in Table 1.

Table 1. Definition of deformation indices using available models

Deformation Index	“Simple” Model	Lehman Model	Panagiotakos Analytical Model	Panagiotakos Empirical Model	Priestley Model
$\Delta_{y,flexure}$	$\phi_y L^2/3$	$\phi_y L^2/3$	$\phi_y L^2/3$	$\phi_y L^2/3$	$\phi_y(L+0.15f_y d_b)^2/3$
$\Delta_{y,shear}$	NA	$V_y L/(0.4E_{c,sec} 0.8A_g)$	NA	0.0025L	$\Delta_{conc, shear} + \Delta_{truss, shear}^{(1)}$
$\Delta_{y,slip}$	NA	$\phi_y L f_y d_b / 8 \sqrt{f_c'}$	NA	$\epsilon_y f_y d_b L / 4 \sqrt{f_c'} (d-d')$	incl w/ $\Delta_{y,flexure}$
$\theta_p$	$(\phi_u - \phi_y) L_p$	$(\phi_u - \phi_y) L_p$	$(\phi_u - \phi_y) L_p^{(2)}$	$\theta_u - \Delta_v / L$	$(\phi_u - \phi_y) L_p$
$\theta_u$	$\Delta_u / L$	$\Delta_u / L$	$\Delta_u / L$	$\Delta_u / L^{(2)}$	$\Delta_u / L$
$\Delta_p$	$\theta_p(L-0.5 L_p)$	$\theta_p(L-0.5 L_p)$	$\theta_p(L-0.5 L_p)$	$\Delta_u - \Delta_v$	$\theta_p(L-0.5 L_p)$
$\Delta_u$	$\Delta_v + \Delta_p$	$\Delta_v + \Delta_p$	$\Delta_v + \Delta_p$	$\theta_u L$	$\Delta_v + \Delta_p$
$L_p$	0.5H	$0.5L(M_u - M_n)/M_n + 1.2(f_u - f_y) d_b / 4 \sqrt{f_c'}$	$0.12L + 0.014f_y d_b$	NA	$0.08L + 0.022f_y d_b$

NA: Not Applicable

<sup>(1)</sup> Details for shear contribution to yield displacement can be found in Priestley et al. (1996).

<sup>(2)</sup> Details for Panagiotakos analytical and empirical models can be found in Panagiotakos and Fardis (2001).

The application of the models (except the Panagiotakos empirical model) requires calculation of yield and ultimate curvatures. At the ultimate point, the contributions to displacements due to shear and anchorage slip, if considered in the model, are lumped in the plastic hinge length. Since in most cases, the proposed plastic hinge lengths are based on reproducing the experimental response, the definitions of yield and ultimate curvatures used by the investigators become important. The Panagiotakos analytical model provides equations for the calculation of yield and ultimate curvatures. We implemented the Mander model (Mander et al., 1988) in the moment-curvature analyses required for the “simple”, Lehman, and Priestley models. Figure 2 shows the moment-curvature response computed for a typical well-confined column. The dashed curve is a bilinear curve fitted to the computed curve, defined by an effective yield point ( $M_n, \phi_y$ ) and failure of the cross-section ( $M_u, \phi_u$ ). The “yield” point ( $M_y, \phi_y'$ ) is defined as the point when the extreme tension steel yields or the strain in the concrete at the extreme compression fiber reaches 0.002, whichever comes first. For any axial load level, the nominal flexural strength,  $M_n$ , is calculated using a rectangular stress block but with the specified (for analytical study) or reported (for experimental data) yield and compressive strengths used without reduction factors. The ultimate curvature is defined as the smallest of the curvatures corresponding to (1) a reduced moment equal to 20% of maximum moment, determined from the moment-curvature analysis, (2) the extreme compression fiber reaching the ultimate concrete compressive strain as determined using the Mander model, and (3) the longitudinal steel reaching a tensile strain of 50% of ultimate strain capacity.

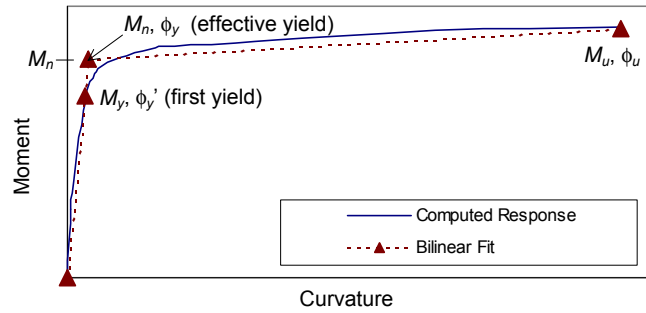


Figure 2. Typical moment-curvature response of a well-confined column

### Inelastic Deformation Capacities from Analytical Models

Using the five models, the sensitivity of the inelastic deformation capacities was studied for cantilevered columns by varying cross section size, aspect ratio, transverse reinforcement amount, and axial load ratio. In one set of analyses, three cross section sizes (305 mm x 305mm, 610 mm x 610 mm, 1220 mm x 1220 mm) were used, with the aspect ratio (cantilever length divided by section depth) held constant at 4. In another set of analyses, aspect ratios were changed from 2 to 10 by varying the column length while the cross section was kept constant. Two levels of transverse reinforcement were considered: the amount required per ATC-32 recommendations and one tenth of the ATC-32 requirement, termed well-confined and poorly-confined, respectively. Two levels of axial load were considered, equal to 0.1 and 0.5 times  $A_g f_c'$ . Material properties were constant for the cases considered; 420 MPa yield strength for both longitudinal and transverse steel and 27.5 MPa for concrete. The longitudinal reinforcement ratio was 1.5% for all cases.

Neglecting minor differences due to cover requirements, the displacement ductility, plastic hinge rotation, and ultimate drift capacities were independent of the cross section size under the constraint of constant aspect ratio of 4. Figure 3 shows how the calculated plastic hinge rotations change with aspect ratio for an invariant cross section. The figure also illustrates the effect of the transverse steel amount, axial load ratio, and the influence of the model used to estimate deformation capacity. Similar plots for displacement ductility and peak drift are available in Inel (2002). The overall trends exhibited by the collection of models lead to the following observations: (a) except for the plastic hinge rotation capacity estimated by the “simple” model, no parameter is invariant with changes in aspect ratio, (b) the sensitivity of the inelastic deformation quantities to the models is obvious; different models can result in substantially different estimates of deformation capacity, (c) the effect of axial load ratio on deformation capacity is clear for the poorly-confined case; deformation capacities are smaller for the high axial load case, even though the ATC-32 compliant transverse steel is greater than for the case of low axial load ratio, and (d) well-confined columns can exhibit substantial calculated deformation capacities, for the cases investigated (axial loads equal to 0.1 and 0.5 times  $A_g f_c'$ ).

Differences in deformation capacities estimated with the models are greater for the high axial load ratio case. The largest differences are observed in the plastic hinge rotation and drift capacities for high aspect ratios, while the largest differences in the displacement ductility capacity are observed for low aspect ratios (Inel, 2002). Key observations related to the individual models are: (a) the “simple” model tends to

provide a lower bound estimate of plastic hinge rotation and peak drift for the well-confined case, (b) the Lehman model is sensitive to the level of confinement. For the poorly-confined case, the deformation capacities estimated by the Lehman model are considerably smaller than those estimated by the Panagiotakos analytical and Priestley models, especially for the low axial load ratio case, (c) the Lehman model is sensitive to the level of axial load. For the well-confined columns with high axial load ratio, plastic hinge rotation and drift capacities estimated by the Lehman model are considerably higher than those estimated by the other models. The reason for this seems to be that the plastic hinge length suggested by Lehman and Moehle (1998) depends explicitly on the axial load ratio while the other models have plastic hinge lengths that are independent of the axial load ratio. For example, for the well-confined case with aspect ratio of 4, when the axial load ratio increases from 0.1 to 0.5, the plastic hinge length estimated by the Lehman model doubles. It should also be noted that although no limitations are identified in the use of the model, Lehman proposed the plastic hinge length equation based on test data for the axial load ratio of 0.1, (d) for the Panagiotakos analytical model, the displacement ductility capacities are nearly independent of the aspect ratio. This contradicts the generally accepted (and experimentally verified by Lehman and Moehle (1998)) trend that displacement ductility capacity decreases as aspect ratio increases. One reason this occurs is that the plastic hinge lengths, estimated by the Panagiotakos analytical model, are considerably smaller for small aspect ratios than those determined by other models such as the Priestley model. Another reason is that the shear displacement contribution to the yield displacement for the Panagiotakos analytical model can be substantial (e.g., the shear contribution may exceed the flexural contribution for an aspect ratio of 2, depending on the axial load ratio), resulting in larger yield displacements. The combination of smaller ultimate displacement capacity and larger yield displacements for small aspect ratios results in smaller ductility capacities; this leads to results counter to the expected trend in displacement ductility capacity as a function of aspect ratio, and (e) the Panagiotakos empirical model tends to estimate higher displacement ductility and drift capacities than the other models for the poorly-confined case.

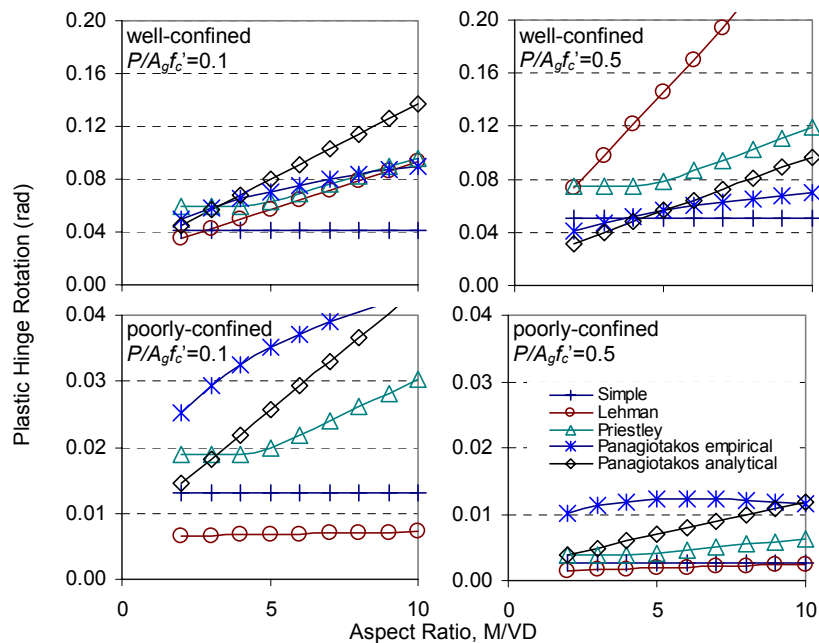


Figure 3. The effect of change in aspect ratio on the inelastic measurement quantities computed using the different models.

In summary, the sensitivity study indicates that none of the inelastic deformation capacity parameters (the plastic hinge rotation, displacement ductility, and peak drift capacities) are a robust, invariant measure of inelastic deformation capacity, for the cases of varying aspect ratio considered. Because the analytical study could not identify a single robust measure of inelastic deformation capacity, the following sections investigate results from experimental tests.

### **Inelastic Deformation Capacities from Experimental Data Set**

The experimental data considered here was obtained from large-scale tests of rectangular reinforced concrete columns subjected to quasi-static reversed cyclic lateral loading, with axial load ratios of varied intensities held constant throughout the tests. Criteria used to establish database were: (1) a rectangular cross section with minimum dimension of 300 mm, (2) at least 8 longitudinal bars, each laterally supported by transverse reinforcement, and (3) minimum aspect ratio ( $M/VD$ ) of 2.5. A total of 23 tests with information required were retained among 29 specimens conforming to these criteria. The retained specimens had aspect ratios ranging from 2.86 to 4.83, axial load ratios,  $P/f_c'A_g$ , ranging between 0.10 and 0.77,  $f_c'$  between 22 and 47 MPa, longitudinal reinforcement ratios ranged between 1.5 and 3.3% of the gross area with yield strength of 430 to 510 MPa.

Experimental data was evaluated by identifying an envelope of the moment at the base of column that includes the applied (actuator) force-deformation plot and the  $P$ - $\Delta$  contribution arising from the applied axial load. That is,  $M = H_{app}L + P\Delta$ , where  $H_{app}$  = applied horizontal force,  $P$  = applied axial load, and  $L$  is column height. It should be noted that secondary moment caused by  $P$ - $\delta$  along the length of member is neglected. The retained specimens had sufficient transverse reinforcement both within and outside potential plastic hinge regions to carry the maximum experimental shear developed during testing based on calculation, with the strengths established using the ATC-32 equations for shear strength. Thus, the inelastic deformation capacity of the specimens was expected to be limited by mechanisms associated with flexural deformation rather than shear strength decay.

The retained data is used to observe effects of axial load ratio on experimentally-determined deformation capacities and as a basis for examining several proposed relations for estimating deformation capacity. The apparent displacement ductility, peak drift, and plastic rotation capacities of the specimens were examined using the identified ultimate displacements in conjunction with the estimated yield displacements and recommended values of plastic hinge length. The word “apparent” signifies data that was obtained or derived directly from the experiments. The ultimate displacements of the columns were determined by review of the measured response data. The ultimate displacement was defined as the maximum displacement corresponding to a 20% reduction of the maximum moment (including  $P$ - $\Delta$  contributions) developed during the experiment. This definition was used by Priestley and Park (1984) among others. Since this definition corresponds to a reduction in lateral strength, it may be assumed that vertical load carrying capacity was maintained throughout and beyond the ultimate displacement capacity as defined here. The use of a 20% drop is arbitrary and is intended to represent a substantial remaining flexural capacity for the confined concrete section. From the data set, it is observed that specimens with ATC-32 compliant transverse reinforcement can achieve a displacement ductility capacity of 6 or more, a

plastic rotation capacity of 0.04 or more, and a drift capacity of 4.5% or more (Inel, 2002).

### Comparison of Apparent and Estimated Deformation Capacities

The apparent inelastic deformation capacities relied upon  $\Delta_y$  and  $L_p$  estimated using available models such as the “simple”, Lehman, Panagiotakos analytical, and Priestley models. These models would have to estimate values of apparent  $\theta_p$  in order to accurately estimate the experimentally determined values of  $\Delta_u$ . This section compares the apparent plastic hinge rotation capacity values with the estimates of  $\theta_p$  according to the four models that use the lumped inelasticity model. The Panagiotakos empirical model is also considered for comparison purposes. For this model, the apparent plastic displacement  $\Delta_{p,apparent} = \Delta_{u,apparent} - \theta_y L$  was compared to the estimated plastic displacement  $\Delta_{p,estimated} = (\theta_u - \theta_y)L$ , where  $\theta_y$  and  $\theta_u$  were computed using the proposed equations. The purpose of the comparisons of this section is to illustrate the reliability of the apparent inelastic deformation capacities determined from the experimental data set, rather than showing the accuracy or inaccuracy of the models. The estimated plastic hinge rotation capacities of the models that use the lumped inelasticity model were calculated as  $\theta_p = (\phi_u - \phi_y)L_p$ .

Comparison between the apparent and estimated deformation capacities shows that differences among the five models are obvious. The ratio of the estimated and the apparent deformation capacities is plotted in Figure 4 against axial load ratio and transverse reinforcement content to identify possible trends. The figure shows that as axial load ratio increases the differences between models become more noticeable. One obvious reason is the differences in the equations for plastic hinge length calculation. The “simple”, Panagiotakos analytical, and Priestley models do not consider the axial load ratio in calculating the plastic hinge length while the Lehman model depends explicitly on the axial load ratio. The effect of transverse reinforcement on the plastic rotation capacity is considered further. As the percentage of ATC-32 transverse reinforcement increases, all models except the Panagiotakos empirical model tend to estimate higher capacities, indicating that the models exaggerate the effect of transverse steel on deformation capacity. The “simple” model tends to underestimate the plastic

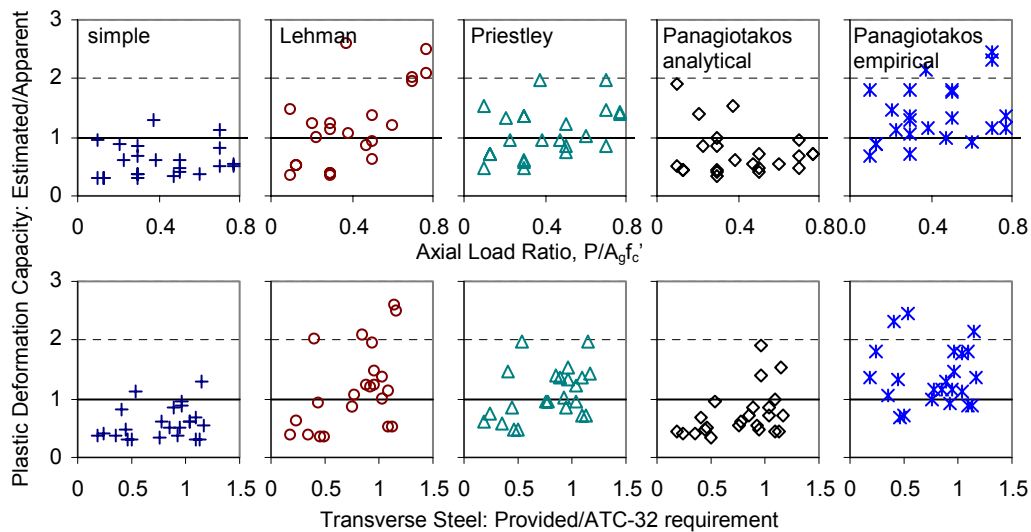


Figure 4. Ratio of the estimated to the apparent plastic deformation capacities of experimental data set vs. axial load ratio and transverse steel content.

deformation capacity while the other models, especially the Lehman and Priestley models, can overestimate the plastic deformation capacity.

## Conclusions

Based on the parametric study of inelastic deformation parameters and the study of the experimental data, the followings were observed: (a) overall, the “simple” model tends to give lower bound estimates of deformation capacity, especially for plastic hinge rotation and drift capacities for columns with aspect ratios of 3 or greater, (b) the parametric study on varying cross section size under constant aspect ratio showed that the displacement ductility, plastic hinge rotation, and drift capacities (as percentage of specimen length) are independent of the cross section scaling when aspect ratio is kept constant. In the parametric study, minor differences relating to cover requirements and nominal bar diameters were neglected, (c) the scatter in the apparent deformation capacities is similar at low and high axial load ratios, (d) plastic rotation capacity was not clearly dependent on axial load ratio when confinement was provided satisfying ATC-32 requirements, (e) analytical models to estimate deformation capacity show large variations, (f) comparison of the apparent and estimated deformation capacities suggests that the analytical models can overestimate deformation capacity, and (g) the analytical models may exaggerate the effect of transverse steel on deformation capacities.

## References

ATC-32, *Improved Seismic Design Criteria for California Bridges: Provisional Recommendations*, Applied Technology Council, Redwood City, California, 1996.

Inel, M., 2002, Displacement-Based Strategies for The Performance-Based Seismic Design of Short Bridges Considering Embankment Flexibility,” *Ph.D. Thesis*, University of Illinois at Urbana-Champaign.

Lehman, D. E., Moehle, J. P., 1998, Seismic Performance of Well-Confined Concrete Bridge Columns, *Pacific Earthquake Engineering Research Center, Report No. PEER-1998/01*, University of California, Berkeley, CA, USA.

Mander, J. B., Priestley, M. J. N., and Park, R., 1988, Theoretical Stress-Strain Model for Confined Concrete, *Journal of Structural Engineering, ASCE*, Vol. 114, No. 8, pp. 1804-1825.

Panagiotakos, T. B., Fardis, M. N., 2001, Deformation of Reinforced Concrete Members at Yielding and Ultimate, *ACI Structural Journal*, Vol. 98, No. 2, pp. 135-148.

Park, R., Paulay, T., 1975, *Reinforced Concrete Structures*, John Wiley & Son, Inc, New York, 769 pp.

Priestley, M. J. N. and Park, R., 1984, Strength and Ductility of Bridge Substructures, *Road Research Unit Bulletin #71*, National Roads Board, Wellington, New Zealand.

Priestley, M. J. N., Seible, F., Calvi, G. M. S., 1996, *Seismic Design and Retrofit of Bridges*, John Wiley & Sons, Inc., New York.